Characteristics of Dual Triangular $\sqrt{3}$ Subdivision

N. A. Dodgson, I. P. Ivrissimtzis, and M. A. Sabin

Abstract. We investigate whether dual triangular $\sqrt{3}$ subdivision can be made practical. We conclude that it has serious drawbacks. Our analysis provides insights into the sorts of problem which occur with subdivision schemes which break symmetry.

§1. Introduction

Dual subdivision schemes are defined in [6] as those where vertices at one level of subdivision map to face centres at the next. Doo-Sabin [3] is the classic example of a dual quadrilateral binary scheme. The principal feature of dual triangular subdivision is that it fails to preserve rotational symmetries. Vertices, which are 6-centres, become face centres, which are only 3-centres. Midedges, which are 2-centres, map to points with no rotational symmetry in the $\sqrt{3}$ case and to 3-centres in the binary case. This loss of symmetry is likely to cause difficulties in deriving a useful dual triangular subdivision scheme. Figure 1 illustrates, however, that, in the regular case, it is easy to construct a dual triangular $\sqrt{3}$ scheme.

This paper was inspired by our work on a complete classification of all possible subdivision schemes [6]. In that work, we classify subdivision schemes in terms of the base mesh and of how mesh primitives (vertices, face centres, midedges) map to one another from one step of subdivision to the next; we identify that it is theoretically possible to have triangular schemes which map vertices at one level to face centres at the next. This paper reports on our investigation into whether such schemes can be made practical.

Curve and Surface Fitting: Saint-Malo 2002
Albert Cohen, Jean-Louis Merrien, and Larry L. Schumaker (eds.), pp. 119–128.

ISBN 0–9728482–1–5

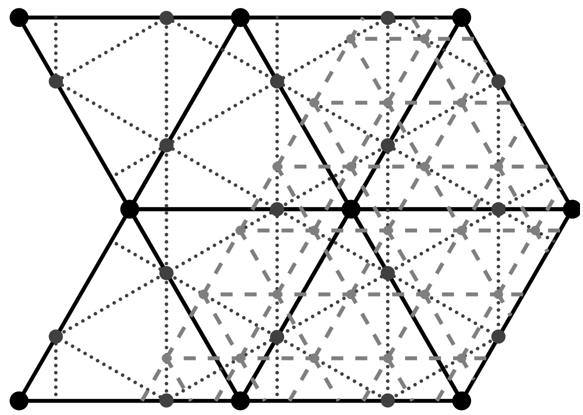

Fig. 1. The geometry of the dual triangular $\sqrt{3}$ subdivision scheme in the regular case. Part of a base regular triangular mesh is shown, with a first level of subdivision (dotted lines) and part of the second line of subdivision (dashed lines).

We chose to investigate dual $\sqrt{3}$ schemes rather than dual binary schemes for two reasons:

1) In dual $\sqrt{3}$, all face centres map to face centres (which is required for a more strict definition of duality than that used in [6]), whereas, in dual binary ($TD(2,0)$ [6]), half of the face centres map to face centres and the other half to vertices.

2) $\sqrt{3}$ provides the slowest refinement of all primal or dual triangular schemes; therefore if dual $\sqrt{3}$ can be made to work, it may offer advantages over binary schemes, whether primal or dual.

The rest of the paper considers the following issues: comparison of dual triangular $\sqrt{3}$ to other $\sqrt{2}$ and $\sqrt{3}$ schemes; factors arising purely from the topology of $\sqrt{3}$ schemes, including the cases of extraordinary faces and extraordinary vertices; factors arising from choice of subdivision mask.

§2. The $\sqrt{2}$ and $\sqrt{3}$ Schemes

Figure 2 illustrates the six types of this slowest form of subdivision. In the notation of Alexa [1] and Ivrissimtzis *et al* [6], these are the $(1,1)$ schemes. The four which preserve symmetry have already received attention: QD [13], QP [15], TP [8], HD [2]. In addition, TP and HD have been combined into a single composite $\sqrt{3}$ scheme [12]. This paper considers the TD scheme. The HP scheme can be expected to have similar characteristics.

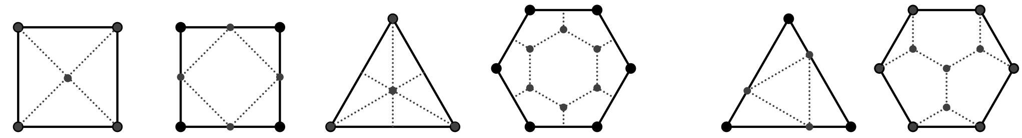

Fig. 2. One cell from each of the $(1,1)$ schemes using the notation of [6]. Q, T and H respectively indicate quadrilateral, triangular and hexagonal base meshes in the regular case. P and D respectively indicate primal and dual schemes. These Q schemes are the $\sqrt{2}$ schemes; while these T and H are the $\sqrt{3}$ schemes.

§3. Topological Considerations

Figure 1 shows that there is no problem with subdividing the regular triangular lattice in a dual triangular $\sqrt{3}$ scheme. Note that, after a single subdivision step, all vertices and all the face centres of both up-pointing and down-pointing triangles become the face centres of left-pointing triangles. After a second subdivision step, they are all face centres of up-pointing triangles. Thus the principal mark points, around which eigenanalysis is performed, are the face centres of up-pointing triangles. This distinction between up- and down-pointing triangles does not occur in primal $\sqrt{3}$, but it does in primal binary schemes (Loop [10] and Butterfly [5]) where face centres of up-pointing triangles become face centres of down-pointing triangles and vice-versa.

A further distinction must be made for dual $\sqrt{3}$ schemes. At each step the triangular lattice is rotated by $\pi/6$. There is a choice at each step as to whether to rotate the lattice by $+\pi/6$ or $-\pi/6$ (see Section 4 for further ramifications of this behaviour). The obvious ways to handle this are either always to rotate in the same direction or to alternate rotation directions. Figure 1 assumes that rotations alternate, given a rotation centre at the face centre of an up-pointing triangle. Different assumptions will produce different limit surfaces. For example, consider a scheme where a vertex affects the position of only the six subdivided vertices nearest to it (i.e. the six vertices which appear on the six edges incident on the vertex). We can show which subdivided vertices are affected by a single original vertex after multiple subdivision steps. Figure 3 shows these approximations to each scheme's support for the two different assumptions, and for Kobbelt's primal $\sqrt{3}$ scheme [8]. It is interesting that the same scheme can produce both a fractal and a polygonal support. A detailed analysis of the support of subdivision schemes can be found in [7].

§4. Extraordinary Faces and Extraordinary Vertices

The scheme can be easily adapted to extraordinary faces (faces with more than three edges) but there are difficulties in extending the scheme to

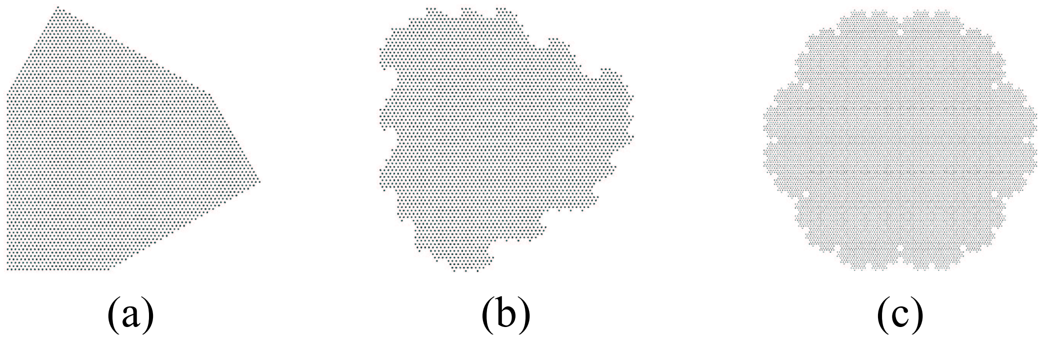

Fig. 3. These diagrams show the vertices in the sixth subdivision step which are affected by a single original vertex. They provide a good approximation to the shape of the support of each subdivision scheme. (a) dual $\sqrt{3}$ assuming alternating rotation directions on alternate steps. (b) dual $\sqrt{3}$ assuming the same rotation direction on every step. (c) primal $\sqrt{3}$ [8]. For more details see [7].

cope with extraordinary vertices (vertices of valence other than six). To explain these difficulties, we note that there are two ways in which a triangular face can map to a triangular face in the refined mesh. In both cases the refined triangular face has edges of length $1/\sqrt{3}$ relative to the original face, but it can be rotated by either $+\pi/6$ or $-\pi/6$ relative to the original face. Call these two types of triangle **C** and **A** (Figure 4(a)). In the regular mesh these correspond to up- and down-pointing triangles. Around an extraordinary vertex or face, the distinctions between up- and down-pointing becomes rather strained, so we use **C** and **A** for clarity.

Around an extraordinary face, all triangles which share an edge with the face will have the same type. It is therefore straightforward to refine an extraordinary face to a face with the same number of edges.

Around any vertex, **C** and **A** triangles must alternate for the scheme to work in a simple way. This can be explained by considering the position of the refined vertex on the common edge of adjacent triangles. If it is positioned so that one triangle is type **C**, then this forces the adjacent triangle to be type **A**. Another manifestation of this can be seen around a regular vertex (Figure 4(b)). Here, every alternate edge has a refined vertex one third of the way along it, while the other edges have a refined vertex two thirds of the way along the edge (as measured from the source vertex). This alternation is a consequence of the symmetry-breaking nature of triangular dual schemes.

For any mesh consisting only of even-valence vertices, **A** and **C** faces can always be made to alternate. Designate an arbitrary face to be of type **C** and the labelling of all other faces is automatic and unique.

Even-valence extraordinary vertices can thus be handled easily. Valence 8 vertices become squares, valence 10 become pentagons, and so on.

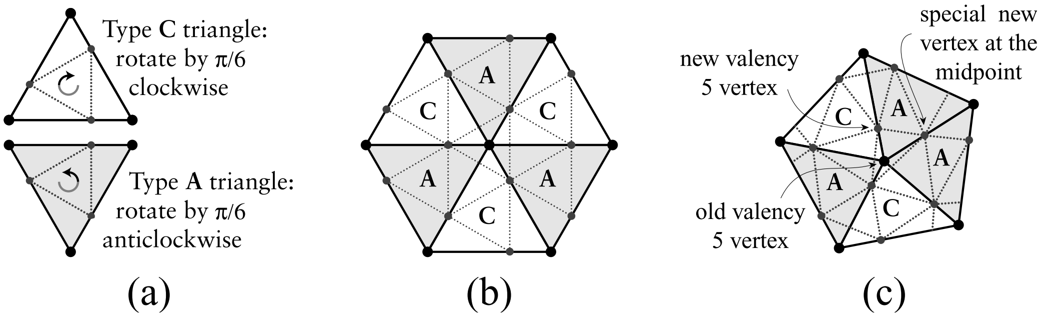

Fig. 4. (a) The two types of triangle: **C** and **A**. (b) Around a regular vertex (or any even valency vertex) the types of triangle alternate. (c) Around an odd valency vertex, it is impossible for the types of triangle to alternate.

Any valence $2k$ vertex refines to a k-sided face. A valence 4 vertex refines to an edge. The difficulty arises with odd-valence vertices. It is impossible to alternate **A** and **C** triangles around such a vertex. There will have to be two triangles of the same type sharing a common edge. One of these triangles will require the refined vertex on the common edge to lie one-third of the way along the edge; the other will require it to lie two-thirds of the way along the edge. The obvious solution is to place this special vertex halfway along the edge, though this compromise does not solve the whole problem. In addition, there is the question of how to connect the refined vertices around the odd-valence vertex. The best that can be achieved is to connect them in such a way as to minimise the number of odd-valence vertices in the refined mesh. Valence 5 and 7 vertices will always leave another vertex of the same valence in the refined mesh. Valence 3 vertices refine to a valence 4 and a valence 5 vertex, the valence 4 vertex vanishing on the next refinement step. Vertices of valence $2k+1$ can refine to a vertex of valence $2k$ and one of valence 7, or can move down the odd valences slowly, if desired, introducing a vertex of valence 8 at each refinement step until they reach the irreducible minimum of valence 7. Figure 4(c) illustrates what must be done for a vertex of valency 5. Note that the precise nature of the refined mesh depends on the labelling of the triangles.

Unfortunately, an odd-valence vertex has an effect beyond its immediate neighbourhood. Consider an odd-valence vertex surrounded by valence 6 vertices, with the next nearest extraordinary vertex some distance away. The inability to alternate **A** and **C** triangles in the 1-ring around the vertex, propagates out to the 2-ring, so that there will be two adjacent triangles of the same type in the 2-ring. By induction, this problem will also be manifest in the 3-ring, the 4-ring, and so on. Indeed, the only way to stop the propagation is by having a second odd-valence vertex intercept the trail of pairs of triangles of the same type (Figure 5). Wherever two triangles of the same type have a common edge, there is a need to place the refined vertex halfway along that edge, and there is a

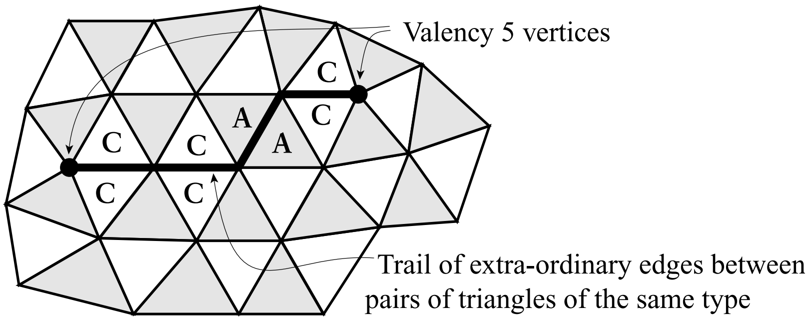

Fig. 5. In a mesh with odd valency vertices, pairs of triangles of the same type will appear. A pair of the same type will appear next to any odd valency vertex and a trail of pairs will propagate out from the odd valency vertex until another odd valency vertex is encountered. Determining a good labelling of the mesh is a global optimisation problem.

special case of the mesh connectivity around the original vertices at either end of the edge.

All of this makes the scheme extremely unattractive for meshes which contain any odd-valence vertices. Lovász [9] proves that it is possible to label the triangles in any triangular mesh with one of two labels (here we use **A** and **C**) so that nowhere are more than two triangles with the same label adjacent. Nürnberger and Zeilfelder [11] have developed an algorithm which can achieve this labelling in under a second for a mesh with a million triangles. We suspect that, given a labelling of the original mesh, a suitable labelling of the refined mesh can be derived, so the labelling need only be done once. This labelling provides some limitation on the problem, but it is clear that the limit surface will depend on the labelling and that many labellings are possible for a given mesh.

§5. Choice of Subdivision Mask

All of the above arises purely out of the geometry and topology of dual triangular schemes, regardless of the choice of subdivision mask. While there are already clear problems inherent in the scheme, we will consider one particular choice of subdivision mask to ascertain if any benefit can be found in pursuing the scheme further. The simplest possible scheme calculates a new vertex as the weighted mean of the two source vertices at either end of its edge. In the general case the weights will be one third and two thirds. For the special case required when two **A** triangles or two **C** triangles meet at an edge, that edge's new vertex will use weights one half and one half. This choice of mask is a triangular analogue of Peters and Reif's simplest (dual quadrilateral $\sqrt{2}$, $QD(1,1)$) scheme [13].

It is possible to perform eigenanalysis [14] around the principal mark point for this scheme. In the regular case, two steps of subdivision lead to

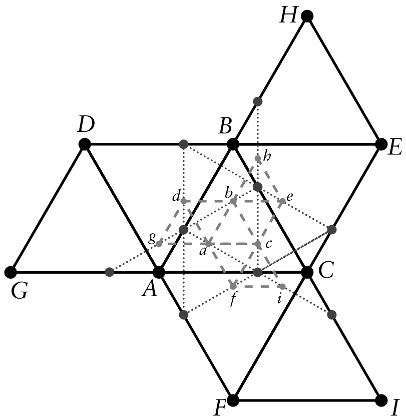

(a)

$$\begin{bmatrix} a \\ b \\ c \\ d \\ e \\ f \\ g \\ h \\ i \end{bmatrix} = \frac{1}{9} \begin{bmatrix} 5 & 2 & 2 & & & & & & \\ 2 & 5 & 2 & & & & & & \\ 2 & 2 & 5 & & & & & & \\ 4 & 4 & & 1 & & & & & \\ & 4 & 4 & & 1 & & & & \\ 4 & & 4 & & & 1 & & & \\ 6 & 2 & & & & & 1 & & \\ & 6 & 2 & & & & & 1 & \\ 2 & & 6 & & & & & & 1 \end{bmatrix} \begin{bmatrix} A \\ B \\ C \\ D \\ E \\ F \\ G \\ H \\ I \end{bmatrix}$$

(b)

Fig. 6. Eigenanalysis: (a) the self-similar region after two steps of subdivision. (b) the associated matrix.

the region of interest shown in Figure 6(a). Note that, while it has three-fold rotational symmetry, it has no reflection symmetry. The eigenvalues of the corresponding matrix (Figure 6(b)) are: $1, \frac{1}{3}, \frac{1}{3}, \frac{1}{9}, \frac{1}{9}, \frac{1}{9}, \frac{1}{9}, \frac{1}{9}, \frac{1}{9}$. This provides necessary conditions for C^1 continuity and proves that the scheme cannot have C^2 continuity (although the second derivative will be bounded). The mask of a double subdivision step is shown in Figure 7. It is clear that this is not divisible along the horizontal principal axis by $(1 + z_1 + z_1^2)$ nor by the equivalent factor along either of the other principal axes. Hence it is not possible to apply Dyn's Laurent polynomial analysis [4] to determine if the scheme meets the sufficient conditions for C^1. It also shows that, in common with primal $\sqrt{3}$, there are no directions for which an extruded polyhedron gives an extruded limit surface. However, it is interesting to note that the scheme can be split into three components (Figure 7) which can themselves each be factorised twice. We are investigating the use of such splits for the analysis of other (primal) schemes. When that analysis is complete, we will be able to apply it to this scheme.

§6. Conclusion

It is possible to construct a dual triangular $\sqrt{3}$ scheme, with some limitations and drawbacks. The advantages of the scheme are that it has:

1) The smallest possible subdivision mask, making computation of new vertices simple and efficient.
2) The lowest possible difference in scale between subdivision levels ($\sqrt{3}$) allowing the finest possible control over refinement level.

$$\frac{1}{9}\begin{bmatrix} 1 & & 2 & & 1 & & & & & & \\ & 2 & & 4 & & 4 & & 2 & & & \\ 2 & & 5 & & 6 & & 5 & & 2 & & 1 \\ & 4 & & 6 & & 6 & & 4 & & 2 & \\ 1 & & 4 & & 5 & & 4 & & 1 & & \\ & 2 & & 2 & & 2 & & & & & \\ & & 1 & & & & & & & & \end{bmatrix} = \frac{1}{9}\begin{bmatrix} 1 & & 1 & & 1 & & & & & \\ & 1 & & 2 & & 2 & & 1 & & \\ 1 & & 2 & & 3 & & 2 & & 1 & \\ & 1 & & 1 & & 2 & & 1 & & 1 \\ & & 1 & & 1 & & 1 & & & \end{bmatrix} + \frac{1}{9}\begin{bmatrix} & & 1 & & & & & \\ & 1 & & 1 & & 1 & & \\ 1 & & 2 & & 2 & & 1 & \\ & 2 & & 3 & & 1 & & 1 \\ 1 & & 2 & & 2 & & 1 & \\ & 1 & & 1 & & 1 & & \\ & & 1 & & & & & \end{bmatrix} + \frac{1}{9}\begin{bmatrix} & & 1 & & 1 & & 1 & & & \\ & 1 & & 1 & & 2 & & 1 & & 1 \\ 1 & & 2 & & 3 & & 2 & & 1 & \\ & 1 & & 2 & & 2 & & 1 & & \\ 1 & & 1 & & 1 & & & & & \end{bmatrix}$$

Fig. 7. At left, the mask of two steps of the simple subdivision scheme. This can be decomposed into a sum of three masks, each of which can be factorised.

3) Simple handling of extraordinary faces and even-valency extraordinary vertices.

Against these advantages are ranged grave disadvantages:

1) For the regular mesh, the scheme can be no more than C^1 continuous.
2) For a mesh containing only 6-valent vertices there are two possible slightly different limit surfaces, depending on the initial labelling of the faces.
3) For a mesh containing only even-valency vertices there is the added choice of how to convert each non-6-valent vertex into a polygon at the first subdivision step; there being two possible configurations at each vertex.
4) For a mesh containing odd-valency vertices, there are serious drawbacks: (i) a global optimization problem must be solved to get a suitable labelling of faces; (ii) there are many possible limit surfaces, (iii) the extraordinary vertices move around (Figure 4(c)) and the extraordinary parts of the grid are polylines (Figure 5) rather than isolated vertices or faces, so making it extremely difficult to perform any analysis the limit surface.

Note that only the first advantage and the first disadvantage are specific to the simple scheme described in Section 5. The other advantages and disadvantages are general to any dual triangular $\sqrt{3}$ subdivision scheme. The fourth disadvantages indicates that dual triangular $\sqrt{3}$ schemes are suitable only for meshes which contain only even-valence vertices. This is a serious limitation. The earlier points in the list show that, even accepting this limitation, the disadvantages outweigh the advantages.

The overarching conclusion is that breaking symmetry is a bad idea. This short investigation has provided evidence of the sorts of things which go awry when symmetry is broken and it provides a useful data point showing one boundary to the domain of usable subdivision schemes.

Acknowledgments. This work has been supported by the European Union, under the ægis of the MINGLE project (HPRN–CT–1999–00117). Thanks to Diena Thompson for typing in the original manuscript.

References

1. Alexa, M., Refinement operators of triangle meshes, Comput. Aided Geom. Design **19** (2002) 169–172.
2. Claes, J., K. Beets, F. van Reeth, A corner-cutting scheme for hexagonal subdivision surfaces, Proceedings of SMI2002: Intern. Conf. on Shape Modelling and Applics., IEEE press, 13–20.
3. Doo, D., and M. Sabin, Behaviour of recursive division surfaces near extraordinary points, Computer-Aided Design **10** (1978) 356–360; reprinted in *Seminal Graphics*, ACM, New York (1998) 177–181.
4. Dyn, N., Analysis of convergence and smoothness by the formalism of Laurent polynomials, in *Tutorials on Multiresolution in Geometric Modelling*, A. Iske, E. Quak, and M. S. Floater (eds.), Springer (2002) 51–68.
5. Dyn, N., D. Levin and J. A. Gregory, A butterfly subdivision scheme for surface interpolation with tension control, ACM Trans. on Graphics **9** (1990) 160–169.
6. Ivrissimtzis, I. P., N. A. Dodgson and M. A. Sabin, A generative classification of subdivision schemes with lattice transformations, preprint, available as Tech. Rep't No. 542, Univ. of Cambridge Computer Laboratory (2002).
7. Ivrissimtzis, I. P., M. A. Sabin and N. A. Dodgson, On the support of recursive subdivision, preprint, available as Tech. Rep't No. 544, Univ. of Cambridge Computer Laboratory (2002).
8. Kobbelt, L., $\sqrt{3}$ subdivision, SIGGRAPH 2000, 103–112.
9. Lovász, L., On decomposition of graphs, Stud. Sci. Math. Hung. **1** (1966) 237–238.
10. Loop, C., Smooth subdivision surfaces based on triangles, MSc dissertation, Univ. of Utah Dep't of Mathematics (1987).
11. Nürnberger, G, and F. Zeilfelder, Lagrange interpolation by bivariate C^1-splines with optimal approximation order, Advances in Comp. Math., to appear.
12. Oswald, P, and P. Schröder, Composite primal/dual $\sqrt{3}$-subdivision schemes, Comput. Aided Geom. Design, to appear.
13. Peters, J., and U. Reif, The simplest subdivision scheme for smoothing polyhedra, ACM Trans. on Graphics **16** (1997) 420–431.
14. Sabin, M. A., Eigenanalysis and artifacts of subdivision curves and surfaces, in *Tutorials on Multiresolution in Geometric Modelling*, A. Iske, E. Quak, and M. S. Floater (eds.), Springer (2002) 69–92.
15. Velho, L., and D. Zorin, 4–8 subdivision, Comput. Aided Geom. Design **18** (2001) 397–427.

N. A. Dodgson
University of Cambridge Computer Laboratory
15 J. J. Thomson Ave, Cambridge, CB3 0FD, UK
nad@cl.cam.ac.uk

I. P. Ivrissimtzis
Max-Plank-Institut für Informatik
Stuhlsatzenhausweg 85, Saarbrücken, D–66123, Germany
ivrissimtzis@mpi-sb.mpg.de

M. A. Sabin
Numerical Geometry Ltd
26 Abbey Lane, Lode, Cambridge, CB5 9EP, UK
malcolm@geometry.demon.co.uk